Journal of ELECTRONIC MATERIALS, Vol. 42, No. 6, 2013
DOI: 10.1007/s11664-013-2512-4

Electrical Properties and Scaling Behavior of MWCNT–Soda Lime Silica Glass

M.H. SHAABAN[1,3] and A.A. ALI[2]

1.—Chemistry Department, Faculty of Science, Tanta University, Tanta, Egypt. 2.—Glass Research Department, National Research Centre, Dokki, Cairo, Egypt. 3.—e-mail: mhani55@hotmail.com

Multiwall carbon nanotube (MWCNT)–soda lime silica glass composites were prepared by the direct mixing method. The dielectric properties of the composites were studied to explore the effect of MWCNT content on the conduction and relaxation mechanisms in such composites. A gradual increase in the direct-current (dc) conductivity σ_{dc} was observed up to 7 wt.% MWCNT, with a sharp increase in σ_{dc} for the 10 wt.% sample. Such behavior was related to the increase of internanotube connections. The correlation between σ_{dc} and the nanotube loading p followed the fluctuation-induced tunneling (FIT) model, which can be described by the equation, $\ln\sigma_{dc} \propto p^{-1/3}$. The alternating-current (ac) conductivity exhibited two distinct regimes: (i) a low-frequency plateau and (ii) a high-frequency dispersion regime. The switchover frequency between the two regimes indicated the conductivity relaxation. The onset frequency shifted to higher frequencies with increasing MWCNT content, which was related to connectivity improvement. Investigating the universality of the ac conductivity of these composites, it was found that the data obtained followed a Rolling scaling model. The obtained master curve revealed that the conductivity relaxation can be considered a temperature-independent process. The frequency dependence of the ac conductivity dielectric constant followed the intercluster polarization model.

Key words: Multiwall carbon nanotubes, soda lime silica glass, MWCNT–glass composites, electrical properties and scaling behavior

INTRODUCTION

Recently there has been great interest in the use of carbon nanotubes (CNTs) in the fabrication of composites. Such interest can be attributed to the outstanding properties that can be achieved when CNTs are used in the manufacture of such composites, which are widely used in many fields. This can be exemplified by the substantial improvements in the mechanical, optical, thermal, electrical, and electrochemical properties of composite materials achieved even at low doping levels.[1–3] Furthermore, CNTs have a great ability to be hosted within polymer matrices[2] or inorganic matrices, such as silicates or metals.[4,5]

The behavior of CNTs was studied by Ebbesen et al.,[6] who reported that the electrical conductivity of individual nanotubes in the majority of cases increased with increasing temperature. The temperature dependence behavior of the electrical conductivity of nanotubes indicated a thermally activated process. The current band theory based on the Wigner–Seitz cell model predicted a gapless semiconductor for graphene. However, this model could not explain the observed thermal behavior.[7] A new band model by Fujita et al.[8] proposed that the normal charge carriers in graphene transport are electrons and holes. The electron (hole) wave packets extend over the carbon hexagon and carry the charges $-e$ or $+e$. Thermally activated electrons or

(Received July 27, 2012; accepted January 19, 2013; published online March 6, 2013)

holes generate the temperature behavior of the conductivity observed in the nanotubes. In multiwall carbon nanotubes (MWCNTs) holes run in shells between the carbon walls. The hole currents depend on the size of the shells, being greatest for the outermost shells.[8]

The increase in the electrical conductivity of MWCNT nanocomposites observed at very low CNT concentrations was attributed to the formation of three-dimensional (3D) conductive networks,[9,10] which are the principle cause of electron transport by tunneling or electron hopping occurring along CNT interconnections. At higher CNT concentrations, conduction may occur by electron hopping from one nanotube to an adjacent one where they are close enough, although they need not touch one another.[11] The conductive paths are due to quantum tunneling effects through the composites, where the distance between the conductive components is such that electron hopping can occur.[12]

Dispersion of CNTs in a polymer can be achieved by three methods:

(i) Direct mixing of the CNTs and the polymer
(ii) Modification of either the polymer matrix or the CNT walls
(iii) Addition of a third component,[13] frequently a surfactant

The third method is the most promising and is used for production of conductive nanocomposites with low percolation thresholds and good conductivity levels.[14]

The method of direct mixing of CNTs with the polymer appears to be the simplest and least laborious procedure to achieve incorporation of CNTs into a polymer matrix. Although it results in inhomogeneity, the agglomerates lead to a decrease of the percolation threshold.[15] Increasing the mixing time can considerably improve the distribution of MWCNTs in the polymer matrix. At concentrations near the percolation threshold, enhancing the mixing time can transform the system from nonpercolated into percolated.[12]

The dielectric properties and conductivity of soda lime silica–MWCNT composites were studied over wide temperature and frequency ranges. The objective of this work is to investigate the effect of the MWCNT content on the conduction and relaxation mechanisms in such composites. The possibility of scaling the frequency-dependent values of the ac conductivity at different temperatures into one single master curve is discussed in an attempt to investigate the dynamics of the relaxation mechanism of such composites.

EXPERIMENTAL PROCEDURES

Preparation of Samples

Commercially available soda lime silicate glass substrates were used, composed of (in mol.%) 72.4 SiO_2, 14.2 Na_2O, 6.36 CaO, 6.0 MgO, 0.5 Al_2O_3, 0.20 K_2O, 0.3 SO_3, and 0.04 Fe_2O_3. Glass powder with particle size between 20 μm and 30 μm was utilized for experimentation. The glass powder was cleaned via ultrasonication in acetone followed by ethanol. The MWCNTs (supplied by Shenzhen NANO tech. Port Co., Ltd., China) were fabricated by catalytic pyrolysis of hydrocarbon, having dimensions of 60 nm to 100 nm in diameter and 5 μm to 15 μm in length. The MWCNTs were dispersed in ethanol using an ultrasonic bath for 2 h. The sonicated MWCNTs were added to the ethanol–soda lime glass powder, then the final mixture was ball-milled in ethyl alcohol using ZrO_2 balls for 12 h. The homogenized mixture was subsequently dried at 40°C in a rotary evaporator and then placed into a hot steel mold and heated up to 200°C, then the mixture was pressed (hot compacted) for 5 min at 20 MPa with subsequent cooling of the mold in air to room temperature. The samples were placed in a muffle furnace at 630°C for 4 h under nitrogen atmosphere. Pressed composite discs with 12 mm diameter and 3 mm thickness were prepared in this way and used for electrical and dielectric measurements.

AC and DC Conductivity Measurements

The samples were coated with colloidal silver paste on both sides and then annealed at 100°C for 2 h to ensure good adherence between the electrode and the sample surfaces. The constructed cell for the electrical measurements consisted of a silica tube surrounded by nickel–chrome wire as a heater. A chromel–alumel thermocouple inside the tube was used for temperature measurements. The ac conductivity was measured by applying the complex impedance technique. A constant ac voltage (V_{rms} = 1 V) was applied to the sample. The current passed through the sample was determined by measuring the potential difference across an ohmic resistor connected in series with the sample by using a lock-in amplifier (Stanford Research System SR510). The lock-in amplifier simultaneously measured the voltage across the resistor and the phase difference ϕ between this voltage and the voltage applied to the sample. Since the voltage drop across the ohmic resistance was in phase with the current I, it could be assumed that ϕ was the phase angle between the voltage drop across the sample and the current I passing through it. The ac conductivity σ_{ac}, the dielectric constant ε', and the imaginary and real parts of the permittivity ε'' were calculated using a computer program. To overcome the effect of humidity, the electrical conductivity was measured under vacuum. Measurements were carried out at temperatures from room temperature (306 K) up to 523 K. Furthermore, the dc conductivity was measured by applying a constant voltage (10 V) and measuring the current, and then Ohm's law was applied to calculate the electrical resistance. The

current was measured using a Keithley type 617 electrometer.

RESULTS AND DISCUSSION

AC and DC Conductivities

The temperature dependence of the dc conductivity σ_{dc} in the measured temperature range (306 K to 523 K) is presented in Fig. 1, showing a linear increase in the dc conductivity with increasing temperature. Such a linear correlation could be explained in the light of the small polaron hopping (SPH) conduction model, which was found to account for conduction in alkali silicate glasses.[16] According to the SPH model, the relation between the electrical conductivity and temperature can be expressed as

$$\sigma_{dc} = \sigma_0 \exp(\Delta E_{dc}/kT), \quad (1)$$

where σ_0 is a constant for a given glass composition, k is the Boltzmann constant, and ΔE_{dc} is the activation energy for dc conduction. The values of ΔE_{dc} and σ_{dc} were obtained by using least-square fitting of the experimental data. The obtained ΔE_{dc} and σ_{dc} values are given in Table I. It is noticed that the activation energy values for dc conduction ΔE_{dc} decrease with increasing MWCNT concentration. A gradual increase in the dc conductivity is observed with increasing MWCNT concentration up to 7 wt.%, beyond which the dc conductivity values increase by several orders of magnitude for the 10 wt.% sample, as shown in Fig. 1. In a composite with low MWCNT concentration, i.e., ≤7 wt.%, previous studies indicated that individual nanotubes in polymer composites were coated by a thick polymer layer.[17,18] This layer was thought to form in the solution phase and was expected to result in poor electrical contact between individual nanotubes, leading to lower effective conductivity. This was related to the electrical pathway, manifested by the internanotube connections, which dominated the macroscopic conductivity. When the MWCNT content was increased beyond 7 wt.%, the number of internanotube connections increased, resulting in many conductive paths. Thus, the substantial numbers of carriers traveling through the entire network followed paths that avoided the larger barriers.[19]

Stehlik et al.[4] assumed that the increase in ion conductivity in CNT–$AgAsS_2$ glass composite may be due to a decrease in the energetic barrier for Ag^+ ions to be transported in the glass network. This could be attributed to the presence of some ions that could travel inside (if some CNTs have open ends or defects in their walls enabling ions to enter the tubes) or along the CNTs.

Kilbride et al.[19] reported that, in polymer–nanotube composites, the polymer acted as a potential barrier to internanotube hopping, indicating that the electrical conductivity was limited by tunneling

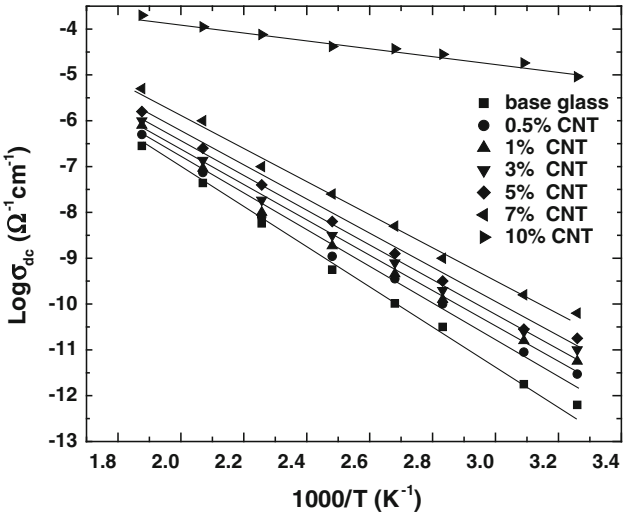

Fig. 1. Log σ_{dc} as a function of 1000/T for different MWCNT contents (x = MWCNT wt.%).

between conductive regions (nanotubes). This behavior was described by the fluctuation-induced tunneling (FIT) model.[20] This model took into account tunneling through potential barriers of varying heights due to local temperature fluctuations, predicting that the conductivity could be described as

$$\ln\sigma_{dc} \propto -w, \quad (2)$$

where w is the gap width. Kribdel assumed that, if the distribution of nanotubes in the polymer host was homogeneous, the dc conductivity σ_{dc} at a given temperature could be described by the behavior of a single tunnel junction, where $w \propto p^{-1/3}$ due to spatial considerations. Thus,

$$\ln\sigma_{dc} \propto -p^{-1/3}, \quad (3)$$

where p is the nanotube loading. The linear correlation observed in Fig. 2 supports the idea that the current is limited by potential barriers between nanotubes and suggests that the dominant mechanism of dc conduction occurs through a fluctuation-induced tunneling mechanism.[19]

The frequency dependence of the ac conductivity at different temperatures for the base soda lime silicate glass sample is depicted in Fig. 3a. At low temperatures, strong temperature dependence is observed. However, this dependence weakens with increasing temperature. This frequency dependence can be represented for each temperature by two straight lines, intersecting at a particular frequency. The value of this intersection frequency increases with increasing temperature, as observed in Fig. 3a. Bruce[21] proposed that the frequency dependence of conductivity for alkali silicate glasses exhibits two slopes and may be expressed by Eq. 4:

$$\sigma_{ac} = A_1\omega_1^n + A_2\omega_2^n, \quad (4)$$

Table I. Calculated values of dc conductivity, ac conductivity, activation energy ΔE_{dc}, and frequency exponent x and y at room temperature for carbon multiwall nanotube (MWCNT)–soda lime silica glass composites

wt.% MWCNT	Log σ_{dc} (300 K) (Ω^{-1} cm^{-1})	Log σ_{ac} (300 K) (Ω^{-1} cm^{-1})	ΔE_{dc} (eV)	x Value at 300 K	y Value at 300 K	$x + y$
0	6.302×10^{-13}	8.912×10^{-10}	0.820	0.970	0.61	1.03
0.5	2.951×10^{-12}	1.479×10^{-9}	0.740	0.950	0.071	1.021
1	5.623×10^{-12}	2.041×10^{-9}	0.713	0.93	0.080	1.010
3	1.023×10^{-11}	2.951×10^{-9}	0.689	0.910	0.092	1.002
5	1.778×10^{-11}	4.168×10^{-9}	0.642	0.900	0.097	0.997
7	6.309×10^{-11}	1.013×10^{-8}	0.540	0.880	0.100	0.980
10	9.124×10^{-6}	2.511×10^{-5}	0.245	0.850	0.122	0.972

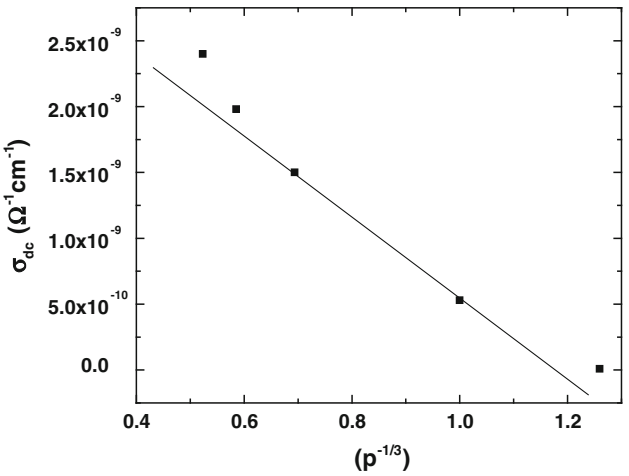

Fig. 2. Relation between MWCNT loading ($p^{-1/3}$) and σ_{dc}.

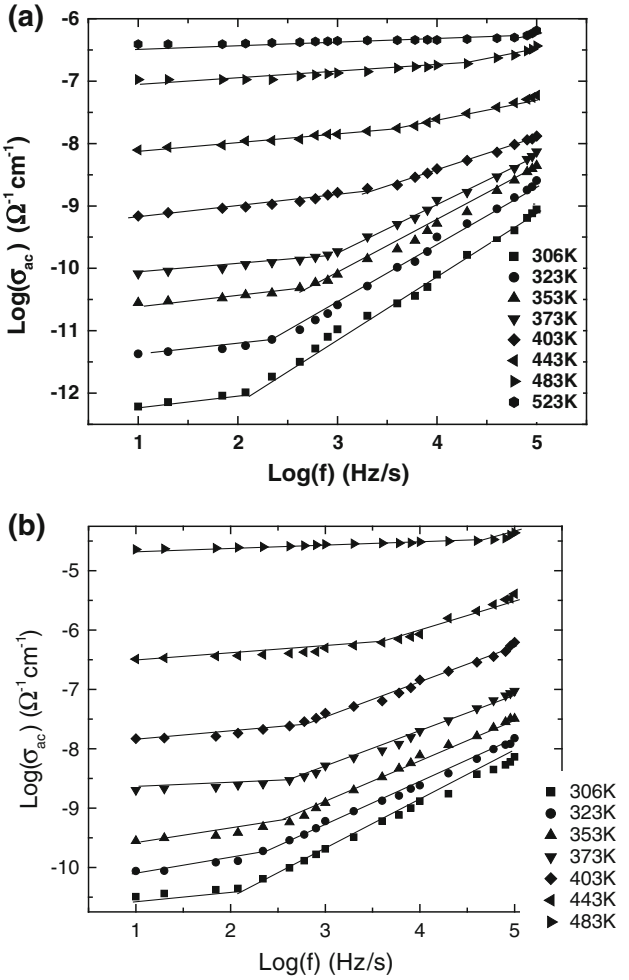

Fig. 3. (a) Relation between ac electrical conductivity (σ_{ac}) and frequency for the base glass. (b) Relation between ac electrical conductivity (σ_{ac}) and frequency for glass containing 7 wt.% MWCNT.

where A_1, A_2, n_1, and n_2 are constants and ω is the frequency.

Figure 3b shows the frequency dependence of the ac conductivity of MWCNT–soda lime silica glass composite (7 wt.% MWCNT) at various temperatures. All the MWCNT–soda lime silicate glass composite samples exhibited similar behavior.

The ac conductivity exhibited two distinct regimes: (i) a low-frequency plateau corresponding to a frequency-independent conductivity $\sigma(0)$, and (ii) at higher frequencies, the ac conductivity increased with increasing frequency (frequency dispersion), following a power-law behavior such that

$$\sigma(\omega) \propto \omega^n, \tag{5}$$

where n is typically $0.6 < n < 1.10$. The real part of the permittivity ε' could be expressed by a power-law decay[22] such that

$$\varepsilon' \propto \omega^{n-1}. \tag{6}$$

Many systems, e.g., polymers, glasses, ceramics, and composites, display similar frequency dependence of conductivity and permittivity, namely Jonscher's universal dielectric response (UDR).[23,24] A number of models have been proposed to interpret this phenomenon. According to the relaxation time distribution (DRT) model, the observed frequency dispersion of the ac conductivity may be related to the presence of inhomogeneity in the glasses, which may be on a microscopic scale with the distribution

of relaxation time (DRT) occurring through a distribution of energy barriers.[25,26] On the other hand, Almond et al.[24] presented a random resistor–capacitor networks model, which represented a heterogeneous microstructure consisting of conducting and insulating regions.[27,28] Thus, at low frequencies a frequency-independent conductivity $\sigma(0)$ behavior was observed (Fig. 3b). The current flowed through the resistors, and $\sigma(0)$ corresponded to one or more percolation paths of resistors across the network. At higher frequencies the resistor–capacitor network exhibited frequency dispersion with clear power dependencies of conductivity and capacitance. The resistor conductivity R^{-1} was frequency independent. However, the conductivity (admittance) of the capacitor ωC increased linearly with frequency. At a sufficiently high frequency, the capacitor admittance was comparable to the resistor conductivity $R^{-1} < \omega C$, and in this frequency range both the resistors and capacitors now contribute to the overall network response.[29]

The onset frequency (ω_o) at which the ac conductivity switched over from the frequency-independent region at low frequency to the frequency-dependent region at higher frequencies implies a conductivity relaxation phenomenon,[25] shifting to higher frequencies with increasing temperature (Fig. 3a, b). The onset frequency ω_o shifted to higher frequencies as the MWCNT content increased, as shown in Fig. 4. The onset frequency ω_o could be defined as the frequency at which $\omega_o = 1.1\sigma_{dc}$. The log onset frequency is plotted as a function of log temperature for the composite containing 7 wt.% MWCNT in Fig. 5. The observed linear relationship suggests a relation of the form $\omega_o = T^q$, where $q = 3.6$, which is approximately equal to that obtained by Jaiswal et al.[30] As stated by Kilbride et al.,[19] in disordered systems, the correlation length λ corresponds to the distance between connections. Sangeeth et al.[31] proposed for disordered systems that the onset frequency scales inversely proportionally to some power of this correlation length. They implied that, at the onset frequency ω_o, the charge carrier travels a distance approximately equal to λ. It travels a shorter distance above the onset frequency, within a well-connected region without difficult hopping processes. The higher value of the onset frequency indicates a shorter correlation length.[31] Accordingly, the observed increase in onset frequency with increasing MWCNT content implies that connectivity was improved with greater MWCNT loading in the composite.[19,31] However, the decrease in onset frequency as the temperature decreased indicates that transport via links in the network was reduced at low temperatures. Accordingly, the value of ω_o could be considered as a useful parameter to probe the extent of connectivity in the system, as well as to optimize the performance of MWCNT composites.

Scaling Model of AC Conductivity

Many attempts have been made at scaling data to investigate the universality of ac conductivity properties in disordered solids. Scaling is the process of forming a set of curves to represent the frequency dependence of some function at different temperatures or concentrations in order to collapse such curves into one single master curve. The dc conductivity and ω_o values are parameters frequently used in scaling methods. The extended pair approximation (EPA) model[32,33] could describe this type of data using the equation

$$\sigma_{ac}/\sigma_{dc} = 1 + k(\omega/\omega_o)^S, \quad (7)$$

where k is added to take into account our rather arbitrary criterion for measuring plots of σ_{ac}/σ_{dc} versus ω/ω_o. All samples showed deviation from this power-law dependence (EPA model), which practically was observed at high frequencies. Therefore, we performed another scaling process for the ac conductivity as a function of frequency. This scaling

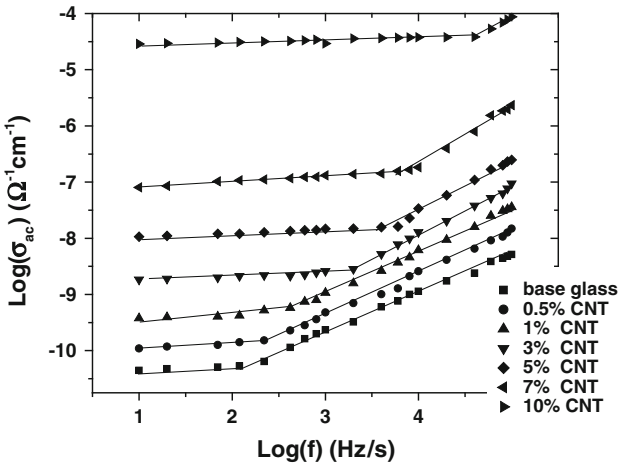

Fig. 4. Relation between ac electrical conductivity (σ_{ac}) and frequency as a function of MWCNT content (x = MWCNT wt.%).

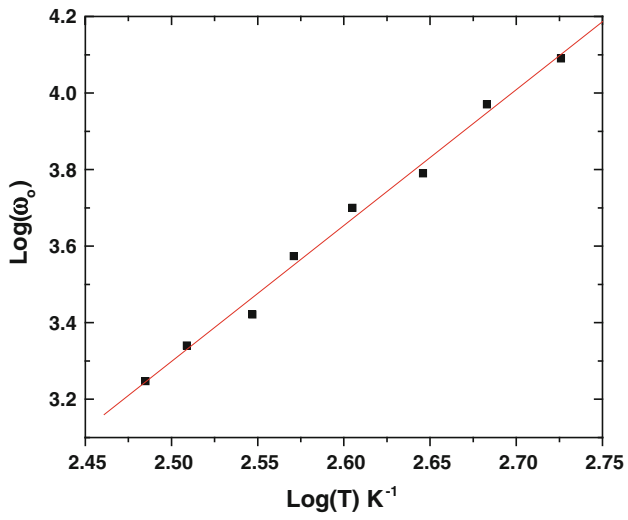

Fig. 5. Relation the Log onset frequency (ω_o) and Log temperature.

model was proposed by Roling et al.,[34] who found that the product $T\sigma_{dc}$ obeyed an Arrhenius relation. They also obtained conductivity master curves for some ionic conducting glasses by using the σ_{dc} value as a scaling parameter. In Fig. 6, we use $\mathrm{Log}(\sigma_{ac}/\sigma_{dc})$ as the y-axis scaling parameter and $\mathrm{Log}(f/T\sigma_{dc})$ as the x-axis scaling parameter. It is clear from Fig. 6 that quite satisfactory collapse of the data for different temperatures onto a single master curve is evident. This behavior indicates that the relaxation in conductivity may be considered a temperature-independent process. In other words, we can say that the quite satisfactory collapse of the data for different temperatures onto a single master curve illustrates well that the dynamic processes occurring at different frequencies need almost the same thermal activation energy. Another indication of these scaled master curves is that all the "Arrhenius" temperature dependence of the conductivity is embedded in the dc conductivity term.[35]

Furthermore, we performed scaling of the ac conductivity data as a function of composition,[36,37] where we used $\log(\sigma_{ac}/\sigma_{dc})$ as the y-axis scaling parameter and $\log(fx/T\sigma_{dc})$ as the x-axis scaling parameter (Fig. 7). We used x (the MWCNT concentration) as an additional scaling factor for the frequency axis. Figure 7 indicates that glasses with 0.05 wt.% to 7 wt.% MWCNT concentration collapsed onto a single master curve. However, the glass with 10 wt.% MWCNT failed to collapse with the other glasses. This indicates differences in the charge carrier conductivity mechanisms between the glasses having <10 wt.% and those having >10 wt.% MWCNT.[37]

The Dielectric Constant ε'

Increase of ε' with increasing temperature is usually associated with a decrease in bond energies, as shown in Fig. 8a. Thus, as the temperature increases, the intermolecular forces weaken and accordingly increase the effects of dipolar polarization and thereby increase the dielectric constant.[38]

Examination of Fig. 8a reveals that the dielectric constant became larger at lower frequencies and higher temperatures, which is expected for oxide glasses and is not an indication of spontaneous polarization.[39] At lower frequencies, charge carriers hop easily out of sites with low free energy barriers in the electric field direction and tend to accumulate at sites with high free energy barriers, leading to net polarization and higher dielectric constant values.[40] However, at high frequencies, the charge carriers can no longer rotate sufficiently rapid, so their oscillation begins to lag behind the field, resulting in a decrease of the dielectric constant.[41] Almond et al.[24] proposed that heterogeneous conductor–insulator materials could be modeled as a large network of conductive and capacitive islands. They concluded that

$$\sigma(\omega) \propto \omega^{\alpha}, \tag{8}$$

$$\varepsilon'(\omega) \propto \omega^{\alpha-1}, \tag{9}$$

where α is the fractional volume of the material occupied by the insulating (dielectric) phase. The power-law exponent n in the UDR in Eqs. 5 and 6 was directly proportional to the α values in these materials. Thus, the increase in conductivity and the decrease in dielectric constant with frequency (Fig. 8a) could be explained in terms of Eqs. 8 and 9.

The frequency dependence of the dielectric constant can be described by the intercluster polarization (IP) model, which implies polarization effects between clusters inside the percolation network.[42,43] The IP model predicts a power-law dependence of ε' and σ_{ac} $[\sigma(\omega)]$ as shown by Eqs. 10 and 11.

$$\sigma(\omega) \propto \omega^{x}, \tag{10}$$

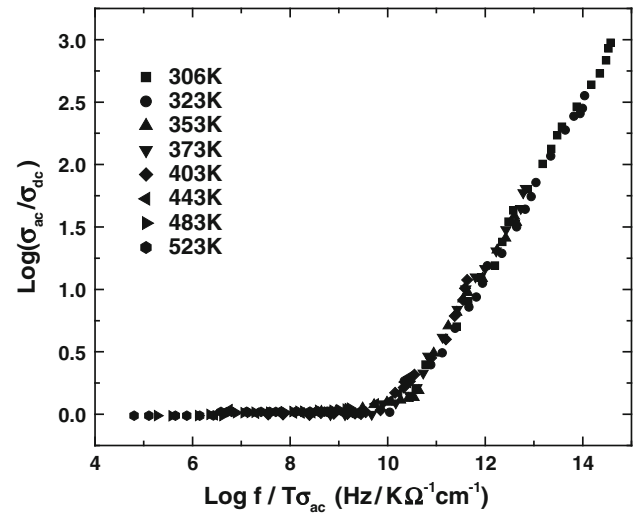

Fig. 6. Relation between $\mathrm{Log}(\sigma_{dc}/\sigma_{ac})$ and $\mathrm{Log}(f/T\sigma_{dc})$ at different temperatures for a sample containing 5% MWCNT.

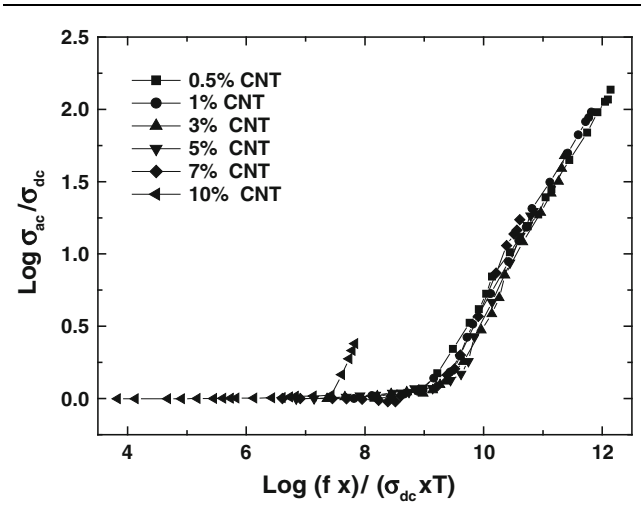

Fig. 7. Relation between $\mathrm{Log}(\sigma_{dc}/\sigma_{ac})$ and $\mathrm{Log}(fx/T\sigma_{dc})$ where x = MWCNT wt.%.

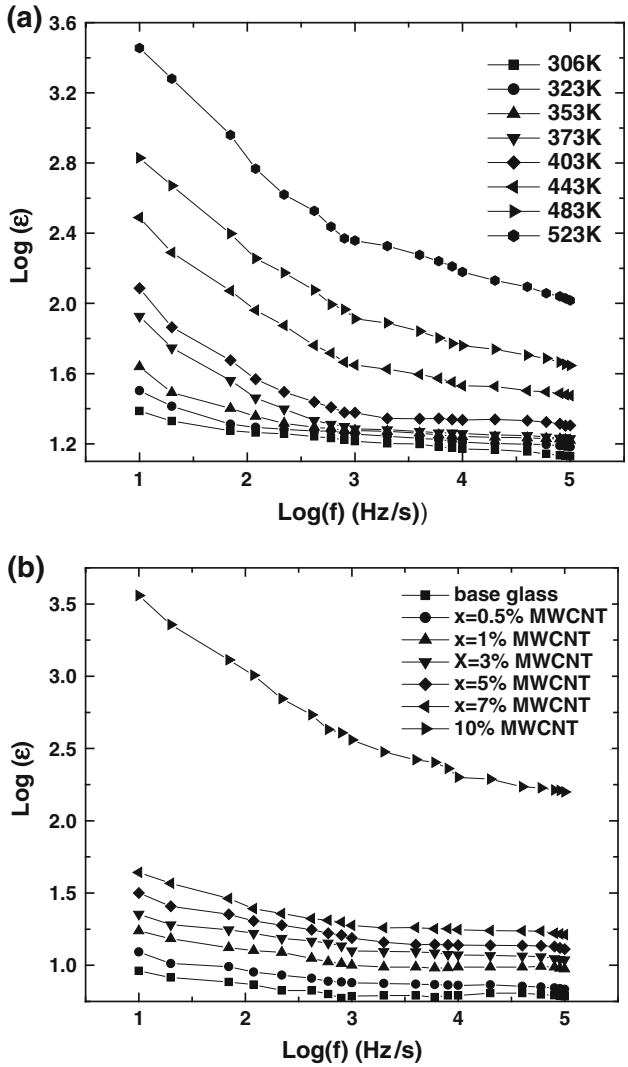

Fig. 8. (a) Relation between dielectric constant (ε') and frequency for a sample containing 7 wt.% MWCNT, at different temperatures. (b) Relation between dielectric constant (ε') and frequency as a function of MWCNT content (x = MWCNT wt.%).

$$\varepsilon'(\omega) \propto \omega^{-y}, \tag{11}$$

where $y = s/(t + s)$ and $x = t/(t + s)$. The critical exponents, x and y, have to satisfy the following condition:

$$x + y = 1. \tag{12}$$

As indicated before, the ac conductivity σ_{ac} shows notable frequency dependence at higher frequencies (Fig. 3). The slope of the curve at room temperature for the sample containing 7 wt.% MWCNT (Fig. 3b) is about 0.88, which is equal to the x value in Eq. 10. From Fig. 8b, the y value for the same sample at room temperature is about 0.100. Thus, $x + y \approx 0.980$, which is approximately equal to that predicted from Eq. 12. A similar behavior was observed for other samples under investigation; the x and y values are given in Table I. Thus, the experimental values satisfactorily obey the general scaling relation $x + y = 1$ predicted by the power law (Eqs. 10 and 11), suggesting that the intercluster polarization (IP) model for the frequency dependence of the dielectric constant[44] could be applied.

Figure 8b shows an increase in the dielectric constant with increasing MWCNT content. Increase in the MWCNT content increased the composite conductivity, which means that the MWCNTs created pathways suitable for migration of more charge carriers. These build up space-charge polarization, leading to an increase in the dielectric constant.[45,46]

CONCLUSIONS

MWCNT–soda lime silica glass composites were prepared by the direct mixing method, and their dielectric properties (ac and dc conductivities and dielectric constant) were investigated. A gradual increase in the dc conductivity σ_{dc} was observed with increasing MWCNT concentration up to 7 wt.%, beyond which the dc conductivity increased by several orders of magnitude for the 10 wt.% sample. This was attributed to the effect of inter-nanotube connections at high MWCNT contents. The results revealed a linear correlation between σ_{dc} and the nanotube loading p as predicted from the relation $\ln\sigma_{dc} \propto p^{-1/3}$. These results suggest that the dominant mechanism of dc conduction occurs through the fluctuation-induced tunneling (FIT) mechanism.

The ac conductivity exhibited two distinct regimes: (i) a low-frequency plateau and (ii) a high-frequency dispersion regime. The switchover frequency between these two regimes implies the onset of conductivity relaxation, which shifted to higher frequencies with increasing MWCNT content. This implies that the connectivity improved with increasing MWCNT loading in the composite.

Investigating the universality of the ac conductivity in these glasses, the Rolling scaling model was applied. The frequency dependence of the ac conductivity at different temperatures or concentrations collapsed into a single master curve, revealing that the conductivity relaxation may be considered a temperature-independent process.

The dielectric constant values increased with increasing MWCNT content. This behavior indicates that the MWCNTs created pathways suitable for migration of more charge carriers. The frequency dependence of the ac conductivity and the dielectric constant could be described by the power-law relations $\sigma(\omega) \propto \omega^{x}$ and $\varepsilon'(\omega) \propto \omega^{-y}$. These results obeyed the general scaling relation $x + y = 1$, suggesting that the intercluster polarization (IP) model could explain the frequency dependence of the dielectric constant.

REFERENCES

1. P.M. Ajayan and J.M. Tour, *Nature* 447, 1066 (2007).
2. K. Kobashi, T. Villmow, T. Andres, L. Häußler, and P. Pötschke, *Smart Mater. Struct.* 18, 035008 (2009).
3. M.J. Andrade, A. Weibel, C. Laurent, S. Roth, C. Estourne's, and Al. Peigney, *Scripta Mater.* 61, 988 (2009).
4. S. Stehlik, J. Orava, T. Kohoutek, T. Wagner, M. Frumar, V. Zima, T. Hara, Y. Matsui, K. Ueda, and M. Pumera, *J. Solid State Chem.* 183, 144 (2010).
5. S.A. Curran, J. Talla, S. Dias, D. Zhang, D. Carroll, and D. Birx, *J. Appl. Phys.* 105, 073711 (2009).
6. T.W. Ebbesen, H.J. Lezec, H. Hiura, J.W. Bennett, H.F. Ghaemi, and T. Thio, *Nature (London)* 382, 54 (1996).
7. G.Ya. Slepyan, S.A. Maksimenko, L. Lakhtakia, O. Yevtushenko, and A.V. Gusakov, *Phys. Rev. B* 60, 17136 (1999).
8. S. Fujita and A. Suzuki, *J. Appl. Phys* 107, 013711 (2010).
9. N.F.A. Zainal, A.A. Azira, S.F. Nik, and M. Rusop, *Nanosci. Nanotechnol.* 1136, 750 (2009).
10. G.D. Seidel and D.C. Lagoudas, *J. Compos. Mater.* 43, 917 (2009).
11. L. Chang, K. Friedrich, L. Ye, and P. Toro, *J. Mater. Sci.* 44, 4003 (2009).
12. M. Chunying, S. Xiangqian, S. Zhou, C. Lei, and X. Zhiwei, *Polymer-Plastics Technol. Eng.* 49, 1172 (2010).
13. N. Grossiord, J. Loos, O. Regev, and C.E. Koning, *Chem. Mater.* 18, 1089 (2006).
14. X.Y. Gong, J. Liu, S. Baskaran, R.D. Voise, and J.S. Young, *Chem. Mater.* 12, 1049 (2000).
15. J.K.W. Sandler, J.E. Kirk, I.A. Kinloch, M.S.P. Shaffer, and A.H. Windle, *Polymer* 44, 5893 (2003).
16. N. Mott, *Philos. Mag.* 19, 835 (1969).
17. R. Murphy, J.N. Coleman, M. Cadek, B. McCarthy, M. Bent, A. Drury, R.C. Barklie, and W.J. Blau, *J. Phys. Chem. B* 106, 3087 (2002).
18. B. McCarthy, J.N. Coleman, S.A. Curran, A.B. Dalton, A.P. Davey, Z. Konya, A. Fonseca, J.B. Nagy, and W.J. Blau, *J. Mater. Sci. Lett.* 19, 2239 (2000).
19. B.E. Kilbride, J.N. Coleman, J. Fraysse, P. Fournet, M. Cadek, A. Drury, S. Hutzler, S. Roth, and W.J. Blau, *J. Appl. Phys.* 92, 4024 (2002).
20. P. Sheng, E.K. Sichel, and J.I. Gittleman, *Phys. Rev. Lett.* 40, 1197 (1978).
21. P.G. Bruce, *Solid State Ionics* 15, 247 (1985).
22. V. Bobnar, P. Lunkenheimer, J. Henberger, A. Loidl, F. Lichtenberg, and J. Mannhart, *Phys. Rev. Lett.* 65, 155115 (2002).
23. A.K. Jonscher, *Nature* 253, 717 (1975).
24. D.P. Almond and C.R. Bowen, *Phys. Rev. Lett.* 92, 15 (2004).
25. R. Murugaraj, G. Govindaraj, and D. George, *Mater. Lett.* 57, 1656 (2003).
26. A.K. Jonscher, *Nature* 267, 673 (1997).
27. D.P. Almond and B. Vainas, *J. Phys.: Condens. Matter* 11, 9081 (1999).
28. R. Bouamrane and D.P. Almond, *J. Phys.: Condens. Matter* 15, 4089 (2003).
29. C.R. Bowen and D.P. Almond, *Mater. Sci. Technol.* 22, 719 (2006).
30. M. Jaiswal, C.S.S. Sangeeth, W. Wang, Y.P. Sun, and R. Menon, *J. Nanosci. Nanotechnol.* 9, 6533 (2009).
31. C.S.S. Sangeeth, M. Jaiswal and R. Menon, *J. Phys.: Condens. Matter*. 21, 072101 (2009).
32. P. Dutta, S. Biswas, M. Ghosh, S.K. De, and S. Chatterjee, *Synth. Met.* 122, 455 (2001).
33. S. Summerfield, *Philos. Mag. B* 52, 9 (1985).
34. B. Roling, A. Happe, K. Funke, and M.D. Ingram, *Phys. Rev. Lett.* 78, 2160 (1997).
35. S.A. Saafan, *Physica B* 403, 2049 (2008).
36. P. Maass, M. Meyer, and A. Bunde, *Phys. Rev.* B51, 8164 (1995).
37. A.A. Ali and M.H. Shaaban, *Bull. Mater. Sci.* 34, 491 (2011).
38. P. Subbalakshmi and N. Veeraiah, *Mater. Lett.* 56, 880 (2002).
39. M. Prashant Kumar, T. Sankarappa, and S. Kumar, *J. Alloys Comp.* 464, 393 (2008).
40. R.S. Kumar and K. Hariharan, *Mater. Chem. Phys.* 60, 28 (1999).
41. P. Bergo, W.M. Pontuschka, J.M. Prison, C.C. Motta, and J.R. Martinelli, *J. Non-Cryst. Solids* 348, 84 (2004).
42. Y. Song, T.W. Noh, S.-I. Lee, and J.R. Gaines, *Phys. Rev. B* 33, 904 (1986).
43. C.S. Yoon and S.I. Lee, *Phys. Rev. B* 42, 4594 (1990).
44. Y.P. Mamunya, V.V. Levchenko, A. Rybak, G. Boiteux, E.V. Lebedev, J. Ulanski, and G. Seytre, *J. Non-Cryst. Solids* 56, 635 (2010).
45. D.L. Sidebottom, *J. Phys.: Condens. Matter* 15, S1585 (2003).
46. P. Syam Prasad, B.V. Raghavaiah, R. Balaji Rao, C. Laxmikanth, and N. Veeraiah, *Solid State Commun.* 132, 235 (2004).